The EMBO Journal (2004) 23, 4353–4364 | © 2004 European Molecular Biology Organization | All Rights Reserved 0261-4189/04
www.embojournal.org

THE EMBO JOURNAL

NSCL-1 and NSCL-2 synergistically determine the fate of GnRH-1 neurons and control necdin gene expression

Marcus Krüger[1], Karen Ruschke[1] and Thomas Braun*

Institute of Physiological Chemistry, University of Halle-Wittenberg, Halle, Germany

To study the role of the bHLH genes NSCL-1 and NSCL-2 in the development of GnRH-1 neurons, we have generated compound mutant mice. Mutant animals die at birth and show a virtually complete absence of GnRH-1 neurons in the posterior parts of the brain at E18.5 and an aberrant morphology of the remaining GnRH-1 neurons in the anterior parts of the brain indicating that NSCL-1 and NSCL-2 might concomitantly control differentiation/migration of GnRH-1 neurons in a cell autonomous manner. To gain further insights into this process, we screened for NSCL target genes using DNA array hybridization and detected necdin, which is deleted in the human Prader–Willi syndrome phenotypically resembling the NSCL-2 mutation. Using chromatin immunoprecipitation and site-directed mutagenesis of the necdin promoter, we demonstrate that NSCLs together with additional cofactors directly control transcription of the necdin gene. NSCL-dependent control of necdin expression might be instrumental for proper neuronal cell differentiation and enable GnRH-1 neurons to migrate.

The EMBO Journal (2004) **23,** 4353–4364. doi:10.1038/sj.emboj.7600431; Published online 7 October 2004
Subject Categories: development; neuroscience
Keywords: differentiation; migration; Prader–Willi syndrome

Introduction

The central regulation of reproductive competence in mammals is mediated by the pulsatile release of GnRH-1 (gonadotropin releasing hormone) from their corresponding hypothalamic neurons (around 800 cells in rodents) (Wray *et al*, 1989) into the portal circulation of the pituitary gland, where it controls the release of gonadotropins and prolactin. Failure of this system will result in infertility and infantile reproductive organs due to hypogonadism and hyperprolactinemia (Wu *et al*, 1997).

GnRH-1-positive neurons originate from the olfactory placode around E11 and consecutively migrate between E11 and E16 on olfactory/vomeronasal axons (Schwanzel-Fukuda and Pfaff, 1989) through the nasal septum and forebrain to the arcuate nucleus (ARC) of the medial hypothalamus. From E17 onwards, GnRH-1 neurons are localized on the ventral side of the cribriform plate in a bilateral continuum between the olfactory bulb through the medial septal nucleus and diagonal band of Broca (DBB) to the preoptic area (POA)/organum vasculosum lateralis terminalis (OVLT) region (Schwanzel-Fukuda and Pfaff, 1989). Most of the GnRH-1-positive neurons project axons to the median eminence, where they secrete the GnRH-1 decapeptide in a pulsatile manner into the hypophyseal blood system (reviewed in Lopez *et al*, 1998). The essential role of the GnRH-1 decapeptide has been highlighted by the analysis of the hypogonadal (hpg) mouse, which lacks physiologically active GnRH-1 due to a truncated gene for the preprohormone (Mason *et al*, 1986).

Numerous genes have been identified to direct development of the neuroendocrine axis (Treier and Rosenfeld, 1996). A particularly interesting group of genes is the bHLH superfamily, which has been shown to play a crucial role in cell fate determination and differentiation during development of the central nervous system (CNS) (Ma *et al*, 1999). The lack of the bHLH-PAS transcription factors Sim1 and Arnt2, for example, leads to the absence of parvocellular and magnocellular neurons within the paraventricular nucleus (PVN) and supraoptic nucleus (SON) of the hypothalamus (Michaud *et al*, 1998; Hosoya *et al*, 2001). Another subgroup of the bHLH family consists of the NSCL-1 (also known as Nhlh1, Hen1) and NSCL-2 (Nhlh2) genes (Lipkowitz *et al*, 1992). Both genes are expressed in largely overlapping patterns in different areas of the CNS and PNS during the embryonic and perinatal stages (Murdoch *et al*, 1999; Kruger and Braun, 2002). NSCL-2−/− mice are hypogonadal and infertile, indicating a requirement of NSCL-2 for proper neuroendocrine development (Good *et al*, 1997; Coyle *et al*, 2002). Furthermore, NSCL-2−/− mice develop adult-onset obesity, suggesting that NSCL-2 is involved in the regulation of energy balance (Nilaweera *et al*, 2002). In contrast, mice lacking NSCL-1 develop normally, are fertile, and show no apparent morphological abnormality (Cogliati *et al*, 2002; Kruger and Braun, 2002), although Cogliati *et al* (2002) reported a decreased lifespan of NSCL-1 mutant mice probably due to a dysfunction of the autonomic nervous system.

The successive acquisition of specific cellular features in the course of differentiation is a prerequisite for numerous morphogenetic events including migration of cells. The ability of cells to undergo targeted migration clearly depends on specialized functions of differentiated cells, which might still be able to proliferate during this process. Hence, faulty differentiation events might result in a loss of migration. For example, a tight link between control of proliferation/differentiation and migration has been revealed for migrating

*Corresponding author. Institut f. Physiologische Chemie, Martin-Luther-Universität, Halle-Wittenberg, Hollystr. 1, Halle, 06097, Germany. Tel.: +49 345 557 3813; Fax: +49 345 557 3811;
E-mail: thomas.braun@medizin.uni-halle.de
[1]These authors contributed equally to this work

Received: 14 April 2004; accepted: 7 September 2004; published online: 7 October 2004

limb muscle precursor cells. Targeted migration of these cells toward the limbs depends on the homeobox gene Lbx1 (Schafer and Braun, 1999), which is involved in the control of proliferation and differentiation of muscle precursor cells (Mennerich and Braun, 2001) clearly demonstrating that proliferation/differentiation and migration are two sides of the same coin.

Here we show that the number of GnRH neurons in NSCL-2 mutants is reduced in the posterior but not in the anterior parts of the brain. Even more striking is the observation that NSCL-1 and NSCL-2 double mutant mice, which die at birth, show a virtually complete absence of GnRH neurons in the posterior parts of the brain, most probably due to cell autonomous defects. Analysis of earlier developmental stages revealed that GnRH neurons form normally in the olfactory area of NSCL-1/NSCL-2 mutants at E14.5 but fail to migrate to the posterior parts of the brain. To begin to decipher the regulatory pathways controlled by NSCL genes, we screened for potential target genes using DNA array hybridization. We found that NSCLs together with additional Lim-domain-only (LMO) cofactors directly control transcription of the necdin gene, which is deleted in the human Prader–Willi syndrome (PWS), characterized by obesity and infertility (MacDonald and Wevrick, 1997).

Results

Generation of NSCL-1 and NSCL-2 lacZ knock-in mice

To analyze the functional role of NSCL-1 and NSCL-2 in neuronal cell formation and to follow the fate of NSCL-1- and NSCL-2-expressing cells, we have inactivated both genes by replacing parts of the second exon encoding the bHLH DNA binding domain with a lacZ cassette (Figure 1A). The generation and the phenotype of NSCL-1 mutant mice have been described before (Kruger and Braun, 2002). Heterozygous NSCL-2 lacZ knock-in mice were fertile and did not show any gross abnormalities. Homozygous NSCL-2 lacZ knock-in mice were clinically normal until puberty when a small penis and small testis became apparent in males. Adult NSCl-2−/− females were characterized by small ovaries and uteri when reared in the absence of males. In addition, we observed adult-onset obesity both in males and females corroborating the previous report (Good *et al*, 1997; Coyle *et al*, 2002).

NSCL-2 and NSCL-1 are expressed in different areas of the developing hypothalamus

In E10.5 heterozygous mutants, NSCL-2 expression was initially found in the subventricular layers of the developing diencephalon (Figure 1C). No obvious alterations of the NSCL-2 expression pattern within the developing hypothalamus were apparent in heterozygous and homozygous mutants between stages E10.5 and E16.5 (Figures 1C and 2A–C), indicating that the fate of NSCL-2-expressing cells remained unchanged during early hypothalamic development. We never found NSCL-2/lacZ signals or NSCL-2 mRNA in Rathke's pouch or in the developing pituitary gland at any embryonic stage (Figure 1Ce–g), whereas postnatally (P10), a weak NSCL-2 gene activity was observed in the anterior lobe of the pituitary gland (Figure 1Ch). It seems likely that earlier reports of an expression of NSCL-2 in Rathke's pouch and the pituitary gland (Good *et al*, 1997) represented a crosshybridization with the highly similar NSCL-1 gene. A strong NSCL-2 activity was observed in hetero- and homozygous embryos between E14.5 and E16.5 in the vomeronasal organ, in the olfactory epithelium, and particularly in the vomeronasal nerve fibers (Figure 1Cb–d) (see Supplementary data). At E18.5, prominent NSCL-2 signals were present in septal areas, in the DBB, within the OVLT region, in the PVN, in lateral areas of the hypothalamus (LH), in the ARC, and in the dorsomedial hypothalamic nucleus (DMH) (Figure 2F–H) (see Supplementary data). Starting at E18.5, NSCL-2−/− mutants exhibited a reduced lacZ activity within the ARC (data not shown), indicating a loss of NSCL-2-dependent cells in this region. In contrast, no obvious changes of NSCL-2 expression were found in the POA (Figure 2I–K) and the DMH areas (data not shown; see Supplementary data), when compared to the decreased expression of NSCL-2 in the ARC. Postnatally, only weak NSCL-2-lacZ activities were detectable in the thalamus (medial habenular nucleus, MHB) and hypothalamus (PVN, ARC, and medial mammillary nucleus (MM), data not shown) both in heterozygous and homozygous NSCL-2 mutant mice.

NSCL-1 gene activity was found, similar to NSCL-2, at E18.5 within several hypothalamic areas including the septal areas, DBB, PVN, ARC, and DMH (Figure 2A–C) (see Supplementary data). In contrast to NSCL-2, we detected NSCL-1 gene activity in the anterior lobe of the developing pituitary gland from E14.5 onwards with a peak at E16.5 (Figure 1Ci–k).

To identify the neuronal cell type(s) in the hypothalamus that expressed NSCL-1 and NSCL-2, we performed double labeling experiments using an antibody against GnRH-1 (LR-1 antibody) and NSCL-1/NSCL-2 reporter gene activities. We colocalized the GnRH-1 protein and NSCL-1 (Figure 2D and E and data not shown) and NSCL-2 gene activities within the same cell between embryonic stages E14.5 and E18.5 (Figure 2G and J and Supplementary data).

The number of hypothalamic NSCL-2-expressing GnRH-1-positive neurons is decreased in NSCL-2 mutants

We next examined whether the lack of either NSCL-1 or NSCL-2 affected the presence of GnRH-1 neurons in adult animals. In NSCL-2 mutant mice, we found a reduction of approximately 30% of GnRH-1 neurons. In addition, a reduction of projecting axons in the median eminence and in the ARC was evident (Figures 2N, O and 3Ae, j), which is in line with previous observations (Good *et al*, 1997). In NSCL-1 mutant mice, we did not observe clinical or morphological alterations related to a disruption of the hypothalamic-pituitary axis or any reduction of the number of GnRH-1 neurons, suggesting a complete compensation of the absence of NSCL-1 by the highly related NSCL-2 gene.

To reveal the distribution of GnRH-1 neurons along the anterior–posterior axis in more detail, we counted all GnRH-1-positive cells per slice (50 μm thick) from septal nuclei and POA to caudal hypothalamic regions: SON retrochiasmatic and lateral hypothalamic area (LH) (Figure 3). The loss of GnRH-1 neurons correlated roughly with the distance that GnRH-1 cells had to migrate from the olfactory placode. The most pronounced reduction was found in the preoptic region including the OVLT (slice numbers 19–25; Figure 3Ac and h), which normally contains the largest number of GnRH-1-positive neurons, and in lateral areas of the hypothalamus

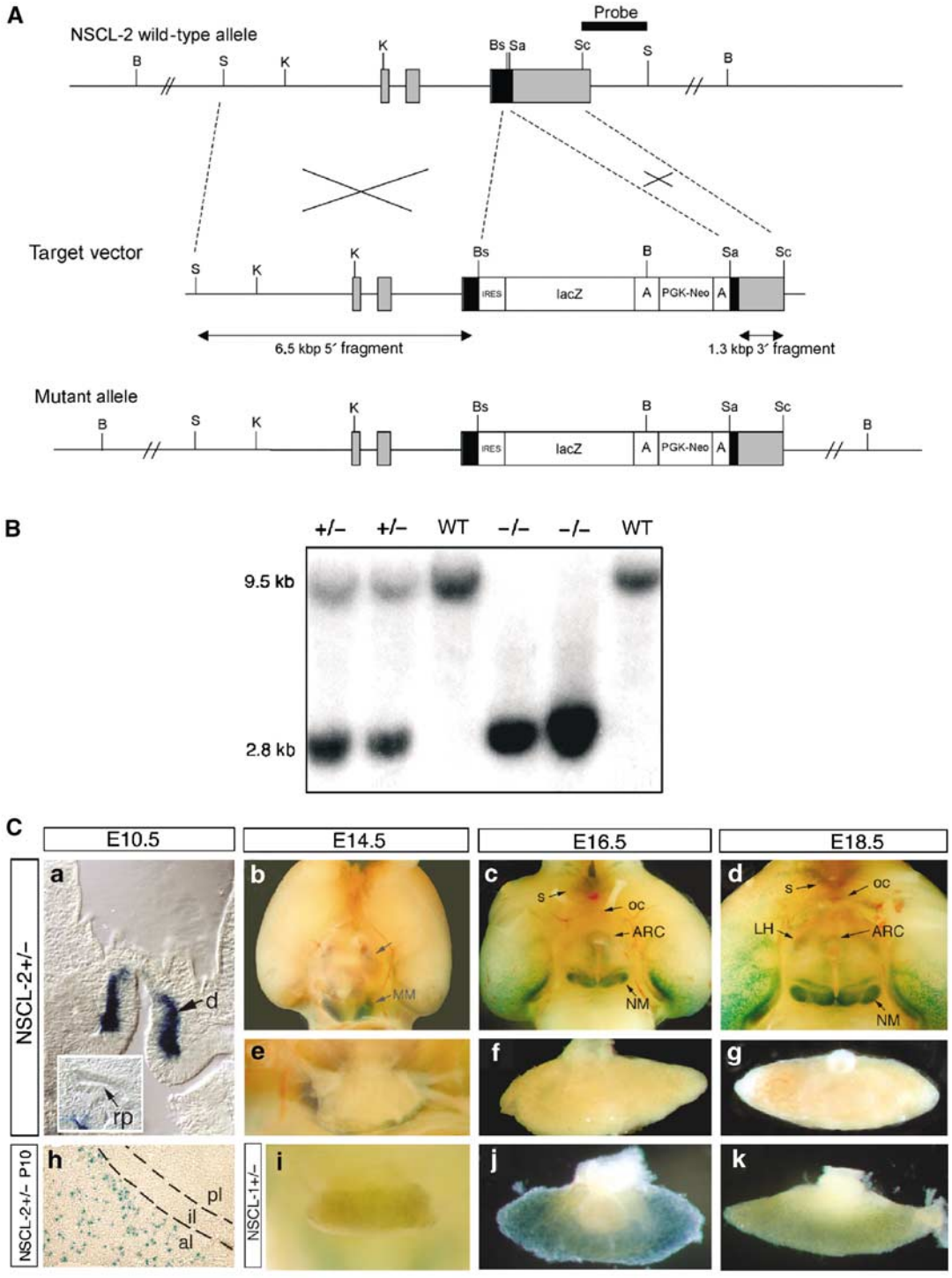

Figure 1 Expression of NSCL-2 and generation of NSCL-2 mutant mice. (**A**) Schematic representation of the NSCL-2 locus (upper row), the targeting vector (middle row), and the disrupted allele generated by homologous recombination (lower row). The IRES-lacZ gene neo resistance cassette (white box) replaced parts of the bHLH region (black box). B: *Bgl*II, Bs: *Bss*HII, K: *Kpn*I, S: *Sal*I, Sa: *Sac*I, Sc: *Sca*I. (**B**) Southern blot analysis of *Bgl*II-digested genomic DNA isolated from NSCL-2 mutant F2 progeny. The probe detected a 9.5 kb fragment in wild-type mice and a 2.8 kb fragment in mutant mice. (**C**) LacZ expression pattern in NSCL-2 heterozygote mice. (a) NSCL-2/lacZ is first turned on in the diencephalons at E10.5. No NSCL-2/lacZ-positive cells were detectable within Rathke's pouch. (b) Ventral view of the developing hypothalamus at E14.5. NSCL-2/lacZ-positive cells are found in the lateral area and in the nucleus mammilaris (arrows in (b)). (c, d) NSCL-2 lacZ-positive cells were present in septal areas, in POA, in the area of the ARC, in the mammilary nucleus, and in the lateral hypothalamus. (e–g) No NSCL-2/lacZ-positive cells were found within the pituitary gland during embryonic development. (h) At P10, NSCL-2 expression is switched on in the anterior lobe of the pituitary gland. (i–k) NSCL-1, in contrast to NSCL-2, is expressed between E14.5 and E18.5 in the anterior lobe of the pituitary gland. ARC: arcuate nucleus, al: anterior lobe, d: diencephalon, il: intermediate lobe, LH: lateral hypothalamus, NM: mammilary nucleus, oc: optic chiasma, pl: posterior lobe, rp: Rathke's pouch, s: septal area.

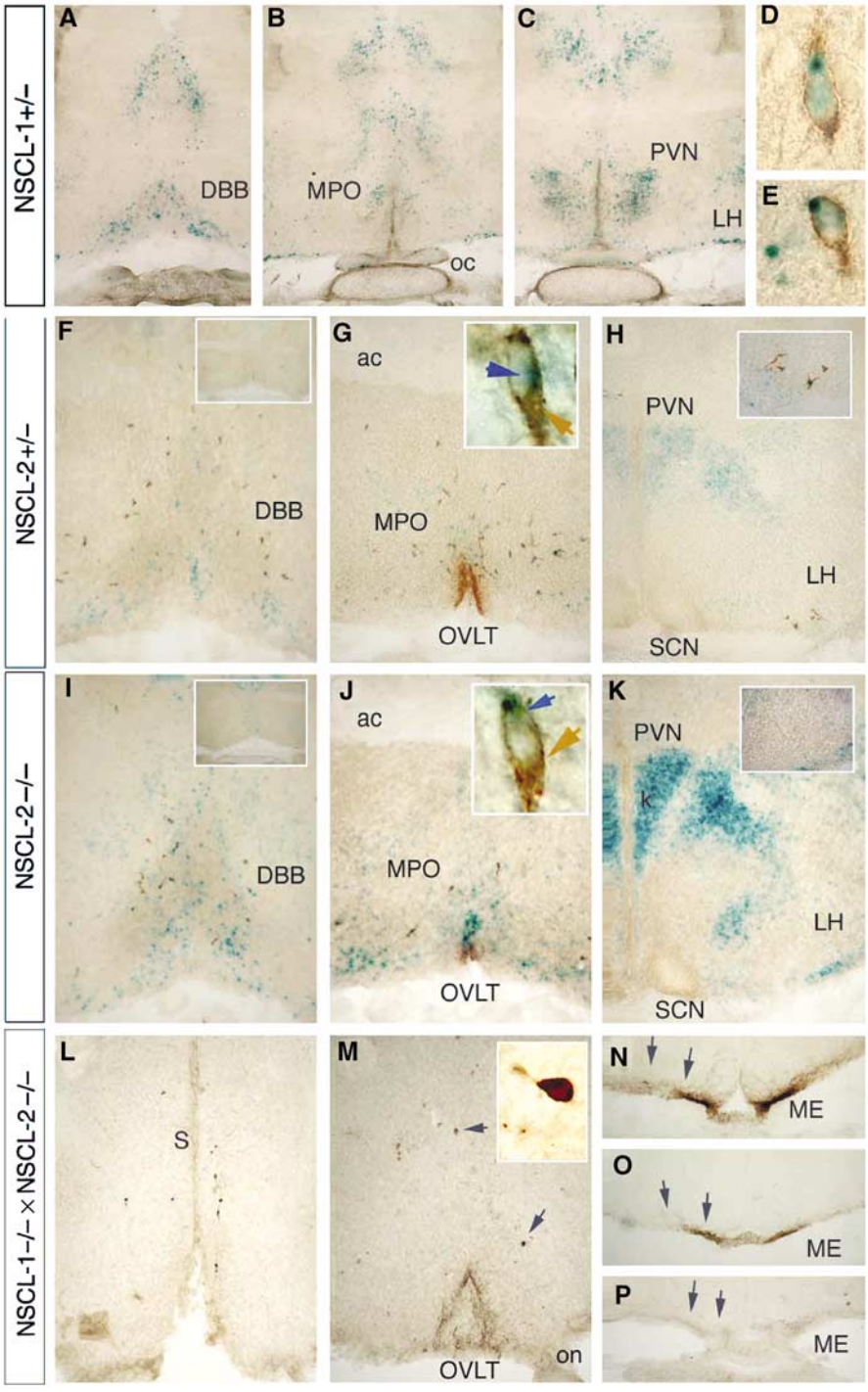

Figure 2 Combined inactivation of NSCL-1 and NSCL-2 leads to a nearly complete absence of GnRH-1 in NSCL-1 × NSCL-2 double mutants. (**A–C**) LacZ staining of NSCL-1 + /− mutants at E18.5. Frontal cryosections (50 μm) reveal NSCL-1-positive cells in POA and dorsomedial areas of the hypothalamus. (**D, E**) GnRH-1 and NSCL-1 are both expressed in the same neurons. (**F–K**) Combined lacZ and GnRH-1 immunostaining of NSCL-2 + /− and NSCL-2−/− mutants at E18.5. Frontal sections through septal area and POA of the hypothalamus of NSCL-2 + /− and NSCL-2−/− mice at E18.5. NSCl-2 and GnRH-1 expressions overlap in the septal area/DBB (F, I), in the OVLT region (G, J), and in the lateral areas of the hypothalamus (H, K). The insets in (G, J) show higher magnifications of double-labeled NSCL-2- and GnRH-1-positive neurons (blue arrow, NSCL-2/LacZ; brown arrow, LR-1 immunostaining). NSCL-2−/− mice display a reduced number of GnRH-1 neurons in POA (J) and a complete absence of GnRH-1 neurons in the lateral areas of the hypothalamus (K). (**L, M**) Immunostaining of frontal cryosections (50 μm) of NSCL-1−/− × NSCL-2−/− mutants at E18.5. (L) Slight increase of GnRH-1-positive cells in the septal areas of NSCL-1−/− × NSCL-2−/− mutant mice compared to heterozygous mice. Double mutant mice lack virtually all GnRH-1 neurons within the DBB and the OVLT (M). Remaining GnRH-1 neurons in NSCL-1/2 double mutant mice (inset in M) show a highly aberrant morphology compared to NSCL-2 + /− mice (insets in G and J). Reduction of GnRH-1 axons in the median eminence of NSCL-2 mutant mice (**O**) and absence of GnRH-1 axons in the median eminence of NSCL-1−/− × NSCL-2−/− (**P**) compared to heterozygous animals at E18.5 (**N**). The arrows in (M) point to a few remaining GnRH-1 neurons in the DBB and OVLT of NSCL-1/2 double mutant mice. ac: anterior commissure, ARC: arcuate nucleus, aPVN: anterior paraventricular nucleus, DBB: diagonal band of Broca, DMH: dorsomedial hypothalamic nucleus, LH: lateral area of the hypothalamus, ME: median eminence, MPO: medial preoptic area, oc: optic chiasma, OVLT: Organum vasculosum lateralis terminalis, PVN: paraventricular nucleus, SCN: suprachiasmatic nucleus.

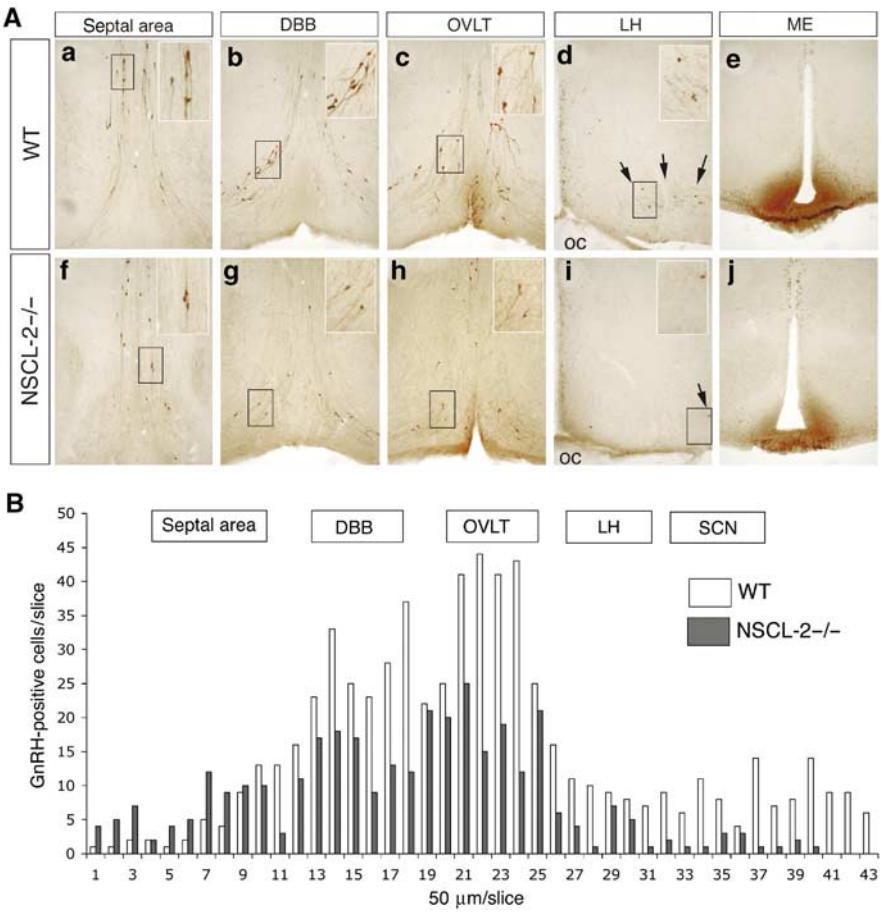

Figure 3 GnRH-1-positive neurons are reduced in the posterior parts of the brains of adult NSCL-2 mutant mice. (**A**) GnRH-1 immunostaining of frontal sections of wild-type (a–e) and NSCL-2−/− animals (f–j). Representative sections through the OVLT (c, h) and lateral areas of the hypothalamus (d, i, arrows). (j) Decreased staining intensity of GnRH-1 fibers in the median eminence of NSCL-2 mutant (j) compared to wild-type mice (e). (**B**) Number of GnRH-1 neurons in different regions of the hypothalamus of wild-type (white bars) and NSCL-2 mutant mice (gray bars). Numbers on *x*-axis indicate the order of individual slices (for abbreviations, see Figure 2).

retrochiasmatically at the level of the SON (slice numbers 27–40; Figure 3Ad and i).

Interestingly, the distribution of the remaining GnRH-1 neurons in mutant mice differed significantly depending on the developmental stage of the embryos. Between E14.5 and E16.5, no significant reduction of GnRH-1 neurons was found in the frontal brain areas of NSCl-2−/− mice in comparison to wild-type animals (Figure 4). At E18.5, we monitored a loss of approximately 30% of GnRH-1 neurons in NSCL-2−/− mice compared with wild-type animals, after counting all GnRH-1 neurons (Figures 3 and 4). Adult NSCL-2−/− displayed a 30% (by 20 weeks of age) and 50% (by 40 weeks of age) reduction of GnRH-1-positive neurons (Figures 3 and 4). During their migration from the olfactory placode to the hypothalamus, GnRH-1 neurons maintained a close contact to NSCL-2/lacZ-positive vomeronasal nerve fibers (see Supplementary data).

Combined inactivation of NSCL-1 and NSCL-2 leads to a dramatic loss of GnRH-1-positive neurons during development

In order to explore potential functional redundancies between NSCL-1 and NSCL-2 for the development of GnRH-1 neurons, double homozygous mutant mice were bred. No obvious morphological malformations occurred in the cortex and in the cerebellum of double mutant mice despite a strong overlapping expression of both genes in these areas (Kruger and Braun, 2002). However, we discovered a severe disruption of the formation of GnRH-1 neurons in NSCL-1 × NSCL-2 double mutants (Figure 2L, M, and P).

Analysis of NSCL-1/2 double mutants at E14.5 revealed a 30% reduction of GnRH-1 neurons when compared to NSCL-1+/− × NSCL-2+/− mutant mice. After 2 days, at E16.5, this loss had increased to 35% and peaked further at E18.5 when only 27% of the normal number of GnRH-1 neurons were left in double homozygous mutants (Figures 2 and 4C). This decrease of 73% was accompanied by a complete absence of GnRH-1-positive fibers within the median eminence (Figure 2P). The severe reduction of GnRH-1-positive neurons in double mutant animals became even more apparent when the local distribution and morphology of remaining GnRH-1-positive neurons were investigated during embryonic development from the olfactory area to the preoptic region within single slices (Figure 4). At E14.5, the majority of GnRH-1-positive neurons in wild-type mice were found in the olfactory area and across the cribiform plate within the olfactory bulb and forebrain. At this stage and location, NSCL-1/2 double mutants showed only a minor reduction of GnRH-1-positive cells, suggesting that the initial proliferation and migration processes of GnRH-1 neurons within the

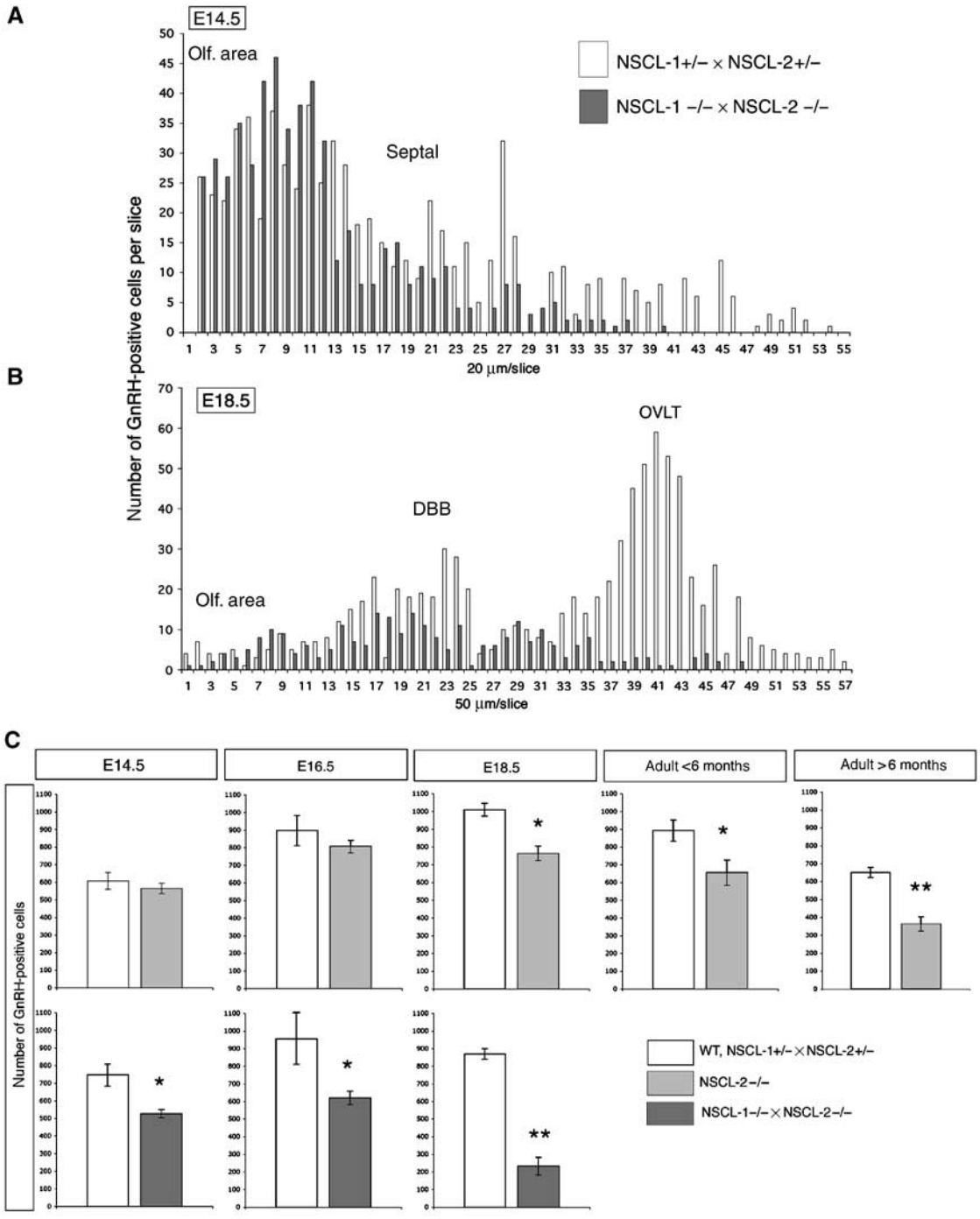

Figure 4 Spatial and temporal distribution of GnRH-1 neurons in NSCL-1 + /− × NSCL-2 + /− and NSCL-1−/− × NSCL-2−/− double mutants. (**A**) Normal or increased numbers of GnRH-1 neurons in the anterior parts of the brains of NSCL-1/2 double mutant mice (gray bars) at E14.5 (sections 1–15) compared to NSCL-1 + /− × NSCL-2 + /− (white bars). GnRH-1 neurons are reduced in the posterior parts of the brains of NSCL-1/2 double mutant mice (sections 20–50) at E14.5. (**B**) Loss of GnRH-1 neurons in the OVLT of NSCL-1/2 double mutant mice (sections 35–50), but normal or slightly increased numbers of GnRH-1 neurons in the anterior parts of the brain (sections 4–14). (**C**) Total numbers of GnRH-1 neurons during development of wild-type (white bars, upper row), NSCL-2−/− (light gray), NSCL-1 + /− × NSCL-2 + /− (white bars, lower row), and NSCL-1−/− × NSCL-2−/− (dark gray) mice. Results are shown as mean ± s.e.m. $^{*}P<0.05$ and $^{**}P<0.01$.

olfactory system were not or only mildly affected (see Supplementary data). The number of nasally located GnRH-1 neurons were not significantly decreased, only those GnRH-1 neurons that had already crossed the cribriform plate and migrated to the ventral forebrain areas were reduced by approximately 30% in NSCL-1/2 double mutants. We did not detect any aberrant location (e.g. in the cortex) of GnRH neurons during the course of our analysis between E14.5 and E18.5. In addition, olfactory and vomeronasal fibers, which are thought to guide migrating GnRH neurons, were correctly located in NSCL-2−/− and double mutant forebrain at E14.5 and stained positive for peripherin (data not shown). At

E18.5, the majority of GnRH-1 neurons had normally completed their journey and migrated to the POA of the hypothalamus such as the DBB and OVLT (Figure 2F and G). In NSCL-1/2 double mutant mice, this process was severely interrupted. Only a small number (ca. 40 GnRH-1 neurons) was able to reach the POA (Figure 2M). These neurons possessed no or only short dendritic processes and did not send axonal projections to the median eminence (Figure 2M and P).

The MAGE gene necdin is a component of the genetic hierarchy controlled by NSCL-1/2

The experiments described above clearly suggested that NSCLs might control the fate of GnRH-1 neurons in a cell autonomous way. We therefore set out to unveil the hierarchy of events that leads to the specification of GnRH-1 cells by NSCLs. We isolated RNA from the hypothalamus of NSCL-1−/− × NSCL-2−/− mutant mice at E18.5 and used the Atlas 1.2 Array System (Clontech) to identify putative NSCL target genes. Among several dysregulated genes, which included genes involved in cell cycle regulation and apoptosis, one particular potential target gene (see Supplementary Table 1), the necdin gene, attracted our attention. The MAGE protein necdin is deleted in the human PWS (MacDonald and Wevrick, 1997), characterized by obesity and infertility, and has been shown genetically to play a crucial role in the development of the hypothalamic-gonadal axis in the mouse. Disruption of the mouse necdin gene results in a loss of 30% of GnRH-1-positive neurons, similar to the phenotype of NSCL-2−/− mutants. In wild-type animals, necdin expression overlaps with NSCL-1/2 expression in discrete regions of the hypothalamus, such as the septal area, POA, and the ARC (Muscatelli *et al*, 2000) (Figure 5A–C). To analyze whether all necdin-expressing regions were similarly affected by the loss of either NSCL-2 or NSCL-1/2, we performed *in situ* hybridization analyses with a necdin antisense probe. We detected a virtually complete absence of necdin expression at the level of the optic chiasma in the hypothalamus of adult NSCL-2-deficient mice, while its expression was only mildly affected in septal and caudal areas (Figure 5D–F). The area, which was devoid of necdin expression, extended considerably at E18.5 in NSCL-1/2 double mutant mice, now including the medial preoptic hypothalamic area and the DBB, where the majority of GnRH-1 neurons are normally located (Figure 5J–L). Hence, at birth, the latest time point, which is currently accessible in these mice, the lack of NSCL-1 and NSCL-2 nearly abolished necdin expression in all areas harboring GnRH-1 neurons that are relevant for establishing the hypothalamic-pituitary axis.

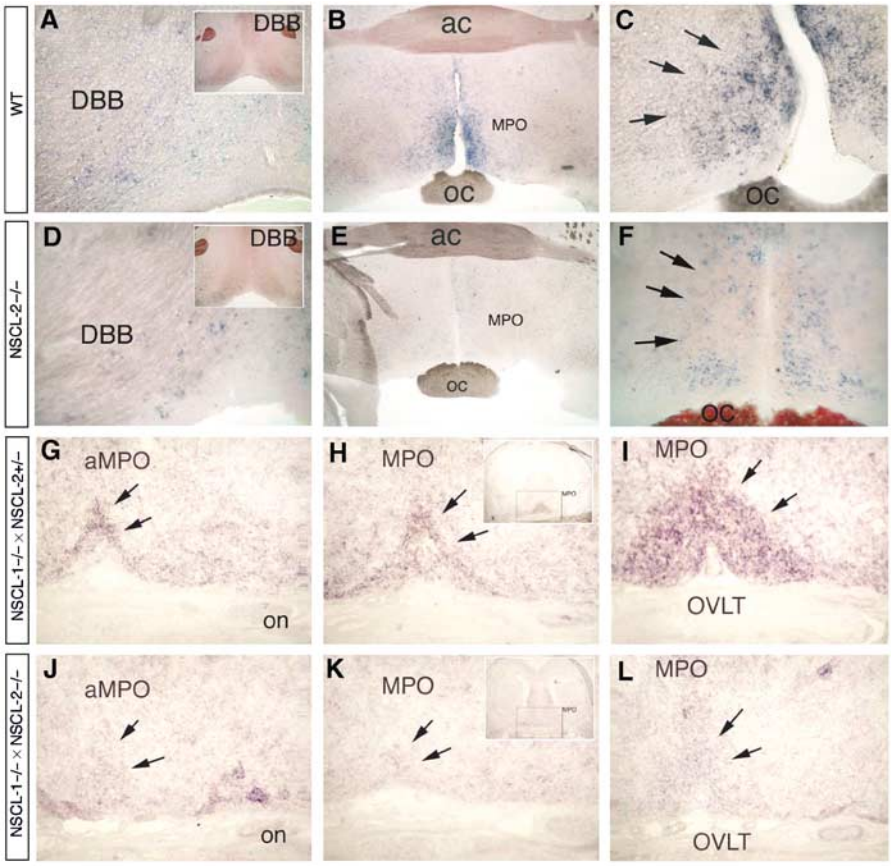

Figure 5 Decreased expression of necdin in NSCL-2−/− and NSCL-1−/− × NSCL-2−/− double mutant mice. *In situ* hybridizations of coronal sections of the hypothalamus of wild-type (**A–C**), NSCL-2−/− (**D–F**), NSCL-1−/− × NSCL-2 +/− (**G–I**), and NSCL-1−/− × NSCL-2−/− (**J–L**) mice at E18.5 with a necdin cDNA probe. Necdin is strongly expressed in the MPO of wild-type (B, C) and NSCL-1−/− × NSCL-2 +/− (G–I) mice at E18.5. Necdin expression is strongly decreased in the MPO of mutant mice (E, F), while no significant changes are discernible in the septal area of NSCL-2−/− mutant mice. Compare (A) with (D). (A, B) and (D, E) are overviews (× 50) of the DBB and MPO. (C) and (F) are enlargements (× 200) of (B) and (E), respectively. Necdin expression is missing in the MPO of NSCL-1 × NSCL-2 double mutant mice (J–L). ac: anterior commissure, DBB: diagonal band of Broca, MPO: medial preoptic area, oc: optic chiasma, on: optic nerve.

The expression of necdin outside the hypothalamus was not affected.

NSCLs directly control transcription of the necdin gene together with additional LMO cofactors

To investigate whether NSCLs directly govern necdin expression via transcriptional control, we studied the proximal regulatory sequences (−844 to +63) of the mouse necdin promoter, which have been shown to be sufficient to direct correct expression of necdin in neuronal P19 cells (Uetsuki *et al*, 1996). We identified two E-box sequences within the mouse promoter at positions −696 (TT**CATGTG**GG) and −548 (CT**CACATG**GA), which contained core binding sites for NSCL-1 and NSCL-2 (Figure 6C). Both proteins carry a very similar bHLH DNA binding domain (98% similarity) with no discernible differences in their *in vitro* DNA binding properties (Lipkowitz *et al*, 1992).

To analyze whether both E-boxes bound NSCL-2 (Figure 6A) and NSCL-1 (data not shown) to a similar degree, we performed electrophoretic mobility shift assay (EMSA) using *in vitro*-translated proteins and radioactively labeled oligonucleotides spanning either the −696 E-box1 or the −548 E-box2 including flanking sequences. As shown in Figure 6A, E-box1 (lane 1) strongly bound NSCL-2, whereas E-box2 (lane 8) served only as a weak substrate for NSCLs. The binding specificity was ascertained using different wild-type and mutant oligonucleotides as competitors (Figure 6A, lanes 2–5 and 9–12). Nonspecific (NS) complexes derived from the reticulocyte lysate were not resistant to competition with mutant binding sites as their specific counterparts.

We then performed chromatin immunoprecipitation (ChIP) experiments to confirm binding of NSCL-2 to the endogenous necdin promoter within its native chromatin structure (Figure 6B). We analyzed both the mouse necdin promoter in the hypothalamic cell line GT1-trk (Mellon *et al*, 1990; Schatzl *et al*, 1997), which contains two E-boxes, and the human promoter in HEK293 cells, which contains three E-boxes (Figure 6C). As shown in Figure 6B, NSCL-2 bound to the endogenous necdin promoter in GT1-trk as wells as in HEK293 cells. No product was recovered when GT1-trk and HEK293 cells were transfected with the myc-tag expression plasmid alone.

We next cotransfected a reporter construct together with an NSCL-2 expression construct in HEK293T cells to explore whether NSCL-2 activates the necdin promoter in cell culture. As shown in Figure 7A, cotransfection with NSCL-2 raised the activity of the necdin promoter nearly 20-fold. Addition of a putative heterodimerization partner of NSCL-2, E12, further stimulated the necdin promoter activity up to 25-fold above background levels.

Several bHLH proteins have been shown to interact with LMO proteins, which do not interact with DNA directly, to transactivate cognate promoters (Johnson *et al*, 1997). We therefore investigated by immuno-co-precipitation whether LMO-1, LMO-2, and LMO-4, which are all found in those areas of the brain that express NSCL-2 (Bulchand *et al*, 2003), interact with NSCL-2. All three LMO-2 proteins formed protein–protein complexes to a varying degree with NSCL-2 in the absence of a DNA-binding site (data not shown). To test whether LMO-1, LMO-2, or LMO-4 indeed collaborated with NSCL-2 *in vivo* to further enhance activity of the necdin promoter, we transfected LMO-1, LMO-2, and LMO-4 together with NSCL-2 and the necdin reporter gene in HEK293T cells. Expression of LMO-2 and LMO-4 but not LMO-1 led to an additional stimulation of promoter gene activity up to 35- and

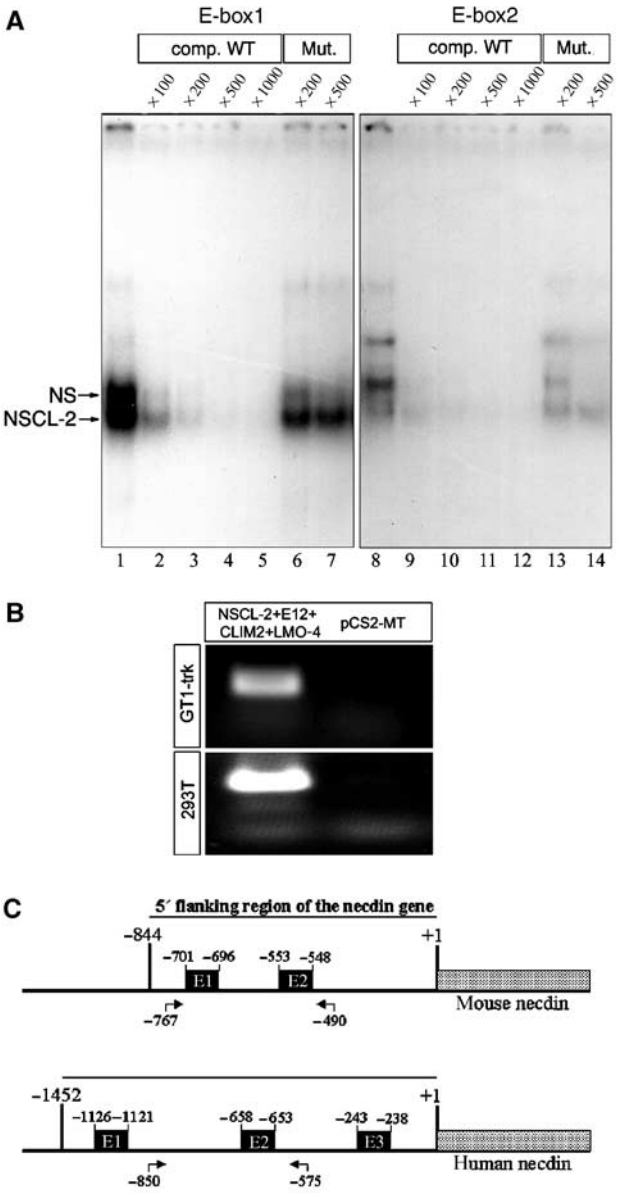

Figure 6 The necdin promoter is a direct target of NSCL-2. (**A**) EMSA with *in vitro*-translated NSCL-2 using E-box1 (lanes 1–7) and E-box2 oligonucleotides (lanes 8–14) derived from the necdin promoter. Specificity of binding was demonstrated by addition of 100- to 1000-fold molar excess of wild-type E-box1 (lanes 2–5) and 200- to 500-fold molar excess of a mutated E-box1 (lanes 6 and 7), and by addition of 100- to 1000-fold molar excess of wild-type E-box2 (lanes 9–12) and 200- to 500-fold molar excess of a mutated E-box2 (lanes 13 and 14). An NS complex that formed with E-box1 and E-box2 was specifically competed with mutated E-boxes (lanes 6, 7 and 13, 14). Unbound oligonucleotides, which were always in excess, are not shown. (**B**) ChIP of the necdin promoter by myc-tagged NSCL-2. Samples of sonicated and purified chromatin isolated from GT1-trk and HEK293 cells transfected with the empty vector pCS2-MT or a combination of NSCL-2, E12, CLIM2, and LMO-4 were immunoprecipitated with the myc-tag antibody. DNAs isolated from immunoprecipitated material were amplified by PCR with primers specific for the human and mouse necdin promoter and resolved on an agarose gel. (**C**) Schematic outline of mouse and human necdin promoters, localization of E-boxes, and position of primers used to identify immunoprecipitated chromatin.

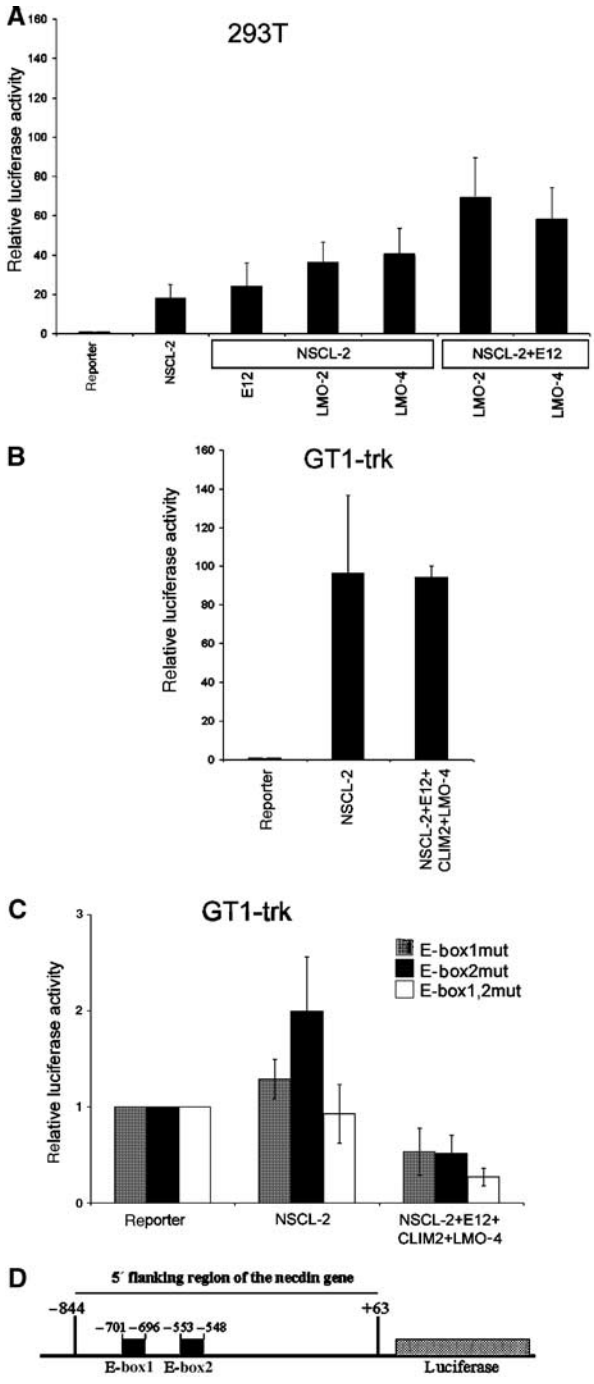

Figure 7 NSCL-2 transactivates the necdin promoter in neuronal and non-neuronal cells. HEK293T cells (**A**) or the hypothalamic cell line GT1-trk (**B, C**) were transfected with necdin-luciferase reporter constructs alone, NSCL-2, or NSCL-2 together with different combinations of cofactors as indicated. The highest activation in HEK293 cells was achieved after cotransfection of NSCL-2 together with the class A bHLH factor E12 and LMO-2 or LMO-4. No further enhancement of necdin promoter activity was observed in GT1-trk cells after addition of E12, LMO-4, or CLIM2. (C) Disruption of E-box1, E-box2, and both E-boxes abolished necdin promoter activity in GT-trk cells. (**D**) Schematic outline of the necdin promoter construct used in transfection experiments and position of mutated E-boxes.

40-fold, respectively, indicating that these cofactors play an important role in NSCL-2-mediated regulation of necdin gene activity. Combined transfection of E12 and LMO-2 or LMO-4 led to a nearly 70-fold activation of NSCL-2 reporter gene activity (Figure 7A). Similar results were obtained when multimerized E-boxes were used as transactivation targets (data not shown).

To further prove that NSCL-2 transactivates the necdin promoter in neuronal cells, we used the hypothalamic cell line GT1-trk. Within this cellular context, we achieved an even higher transactivation of approximately 100-fold (Figure 7B). In contrast to the results obtained in HEK293 cells, supplementation of additional components of the NSCL-2 transcriptional complex (i.e. E12, LMO-4, and CLIM2) in GT1-trk cells did not lead to a further enhancement of necdin promoter activity, indicating that GT1-trk cells contain a sufficient concentration of all the necessary components to allow NSCL-2 to assemble an active transcriptional complex. Finally, we mutated the two E-boxes present in the mouse necdin promoter either alone or in combination by site-directed mutagenesis to demonstrate that transactivation of the necdin promoter by NSCL-2 was indeed mediated by the identified E-boxes. As expected, mutation of either E-box led to virtually complete inactivation of the necdin promoter (Figure 7C) irrespective of the presence or absence of additional components of the NSCL-2 transcriptional complex.

Discussion

NSCL-1 and NSCL-2 synergistically determine GnRH-1 neurons

Our findings suggest that NSCL-1 and NSCL-2 have overlapping functions for the specification of GnRH neurons, since the combined knockout led to a virtually complete absence of GnRH neurons in the posterior parts of the brain. Redundancy between different bHLH genes for the determination of specific cell types has been described before (Schwab *et al*, 1998) although the NSCL-1/2 double knockout has some distinctive features: (i) It affects a comparatively small cell population that comprises only a couple of hundred neurons. (ii) Despite a strong and lasting coexpression of NSCL-1 and NSCL-2 during the early steps of neurogenesis in virtually all cells of the sensory system, the double mutants lack any defects during development and any obvious major malformations in CNS structures such as the cortex and cerebellum (Cogliati *et al*, 2002; Kruger and Braun, 2002). (iii) NSCL-1-deficient mice do not seem to have any defects whatsoever in the development of GnRH-1 neurons and the sensory system. In contrast to the lack of NSCL-2, which can be only partially compensated by NSCL-1, NSCL-2 seems to balance the absence of NSCL-1 entirely. The current data suggest that all cells that express NSCL-1 also express NSCL-2, but not all cells that express NSCL-2 contain NSCL-1. Alternatively, it is possible that both transcription factors are coexpressed in all GnRH neurons but are incapable of full functional compensation. Nevertheless, this option seems less likely given the very high sequence similarity of both proteins and the equivalence of both proteins in several functional assays.

The severe reduction of GnRH-1 neurons in NSCL-1/2 mutant mice is most likely caused by a cell autonomous migration defect

In principle, it is possible that the reduction of GnRH-1 neurons in NSCL-2 and NSCL-1/2 mutant mice is either due

to a cell autonomous defect or is caused indirectly by shortcomings in neurons that guide or otherwise regulate GnRH-1 cells. We have clearly shown that NSCL-1 and NSCL-2 are both expressed in GnRH-1 neurons. The projections of vomeronasal nerve fibers, which are thought to guide migrating GnRH-1 cells, were normal in NSCL-1/2 double mutants based on lacZ staining and expression of peripherin and NCAM. Similarly, no obvious alterations within olfactory and forebrain areas, with the exception of the lack of GnRH-1-positive cells, were detected when double homozygous animals were compared to heterozygous and double heterozygous animals using the lacZ reporter genes located within the NSCL-1 and NSCL-2 loci, again supporting the idea of a cell autonomous phenotype.

Interestingly, the initial generation of GnRH-1 neurons was not affected in NSCL-2 and NSCL-1/2 mutant embryos. Only those GnRH-1 neurons that have already crossed the cribriform plate and migrated to the ventral forebrain were reduced from the early developmental stage onwards. This tendency became more pronounced during later development so that virtually no GnRH-1 neuron was present throughout the POA at E18.5. These results suggested that NSCL-1/2 mutant GnRH-1 cells do not reach a stage that enables them to migrate past the cribriform plate. In further support of this hypothesis, we observed that the low number of NSCL-1- and NSCL-2-deficient GnRH neurons, which managed to enter the POA, showed an aberrant morphology, with only short processes, a clear indicator for deviant differentiation. In addition, NSCL-1 and NSCL-2 are expressed exclusively in postmitotic neurons throughout the CNS excluding a decisive role in early determination of GnRH cells. Instead, NSCLs seem to control neuronal differentiation steps that follow the foundation of this neuronal lineage. Most importantly, the ability of GnRH-1 neurons to migrate might be seen as a result of differentiation events that enable targeted movement of cells.

We did not observe a misguided migration of GnRH-1 neurons to inappropriate destinations as seen in other mutations affecting migration of GnRH-1 neurons. For example, overexpression of glutamic acid decarboxylase-67 (GAD-67) in GnRH-1 neurons led to a misdirection of GnRH-1 neurons into the cortex (Heger *et al*, 2003). Another example concerns the inactivation of the Ebf-2 transcription factor, which has been shown to result in a loss of migrating GnRH-1 neurons and a lack of immunoreactive fibers in the median eminence at P0 (Corradi *et al*, 2003). Ebf2−/− mice show no changes in the early appearance of GnRH-1 neurons but an abnormal retention of GnRH-1 neurons in the nasal cavity, where these neurons seem to degenerate eventually. In contrast to GAD-67 overexpression, which affects the structures that guide GnRH-1 neurons, cell autonomous defects seem to prevail in Ebf2−/− mice and NSCL-1/2 double mutants. Further studies will unveil the functional relationship between these genes.

Necdin is a direct target gene of NSCLs and might mediate NSCL-dependent differentiation and inhibition of cell proliferation

A hallmark of NSCL genes is their expression in postmitotic neurons and the inhibition of cell proliferation in various assays (K Ruschke *et al*, unpublished observations). The identification of necdin as a potential target gene of NSCLs reflects this function since necdin and other members of the MAGE family have been shown to induce differentiation and inhibit cell proliferation (Taniura *et al*, 1999; Kobayashi *et al*, 2002; Tcherpakov *et al*, 2002). The observed reduction of necdin within the medial preoptic nucleus of NSCL-2 mice as well as the severe reduction of necdin expression in the POA of the hypothalamus in NSCL-1/2 double mutant mice met requirements for an NSCL target gene. We reason that MAGE proteins and necdin in particular might be instrumental for NSCLs to inhibit cell cycle progression of neuronal cells and to promote their differentiation (Yoshikawa, 2000).

The human necdin gene maps to chromosome 15q11–13, which is deleted in patients with PWS (Jay *et al*, 1997; MacDonald and Wevrick, 1997). The major symptoms of PWS are obesity and hypogonadism, which resemble the NSCL-2 knockout phenotype. In the mouse, targeted mutation of the necdin gene resulted in a loss of some hypothalamic neurons including GnRH-1-positive neurons (−30%) and behavioral alterations, which are reminiscent of human PWS (Muscatelli *et al*, 2000). Necdin belongs to the MAGE family of cellular regulatory factors, which comprises a large number of genes (Barker and Salehi, 2002). Since the reduction of GnRH-1 neurons observed in necdin-deficient mice is not as severe as in NSCL-1/2 double homozygous mice (Muscatelli *et al*, 2000), it is not unlikely that other members of this large family, which might be affected by the absence of both NSCL-1 and NSCL-2, partially compensate for the lack of necdin. This assumption is also supported by differences between different necdin knockout stains with phenotypes ranging from virtually normal to early postnatal lethality (Gerard *et al*, 1999; Tsai *et al*, 1999; Muscatelli *et al*, 2000). It seems possible that some PWS patients who were diagnosed based on their clinical appearance and who lack a mutation in the classical PWS locus might instead suffer from an NSCL mutation.

To prove that necdin is indeed a direct target gene of NSCLs and not downregulated due to secondary mechanisms or an absence of necdin-expressing cells, we analyzed the promoter of the necdin gene. Using a transient transfection assay in the non-neuronal cell line HEK293 and the hypothalamic cell line GT1-trk, we demonstrated that NSCL-2 together with additional cofactors stimulated the promoter up to 100-fold. Moreover, we localized two E-boxes within the mouse promoter, which strongly bound NSCL-2 (and NSCL-1) *in vitro* in band shift experiments and together with LIM domain proteins conferred NSCL-dependent activity to a basic promoter. The same E-boxes also mediated binding of NSCL-2 to the endogenous necdin promoter within its native chromatin structure *in vivo* as indicated by ChIP experiments. Finally, mutations of either E-box disrupted necdin promoter activity completely, demonstrating the crucial importance of these regulatory elements for transcriptional regulation. In our view, these results provide unequivocal evidence that NSCLs can directly activate the necdin promoter.

Our data support a model in which NSCLs in combination with E12 and LMOs control expression of necdin in a limited subset of hypothalamic neurons, in particular in GnRH-1 neurons. Since necdin induces neuronal cell differentiation and inhibits cell proliferation, NSCL-driven necdin expression might allow GnRH-1 neurons to reach a new stage of differentiation, enable these cells to cross the cribriform plate,

project axons to the median eminence, and complete their cellular program.

Materials and methods

Mice

The generation of NSCL-1 knockout mice has been described before (Kruger and Braun, 2002). The targeting vectors to obtain NSCL-2 knockout mice were constructed by insertion of a 6.5 kbp *Sal*I–*Bss*HII fragment derived from the 5′ region of the NSCL-2 gene comprising the first exon and a part of the second exon into the vector pWH9 in front of an internal ribosomal entry site, the coding region of the lacZ gene and the neomycin resistance cassette. A 1.3 kbp *Sal*I–*Bss*HII fragment from the 3′ region of the NSCL-2 gene was inserted behind the selection cassette to generate a 3′-homology fragment. The recombination vector replaced parts of DNA binding bHLH region by lacZ and neomycin genes. Electroporation and selection of J1 ES cells were performed as described previously. To identify correctly targeted clones, a 3′ external probe (1.3 kbp *Sac*I/*Sca*I fragment) was used to detect a 9.5 kbp *Bgl*II fragment in the wild-type allele and a 2.8 kbp fragment in the mutant allele by Southern blot hybridization.

Histology and immunohistochemistry

For immunohistochemical stainings, mice were transcardially perfused with phosphate-buffered saline (PBS) followed by 4% paraformaldehyde. After perfusion, the brains were removed and postfixed overnight at 4°C in the same fixative. To obtain 50 μm vibratome sections, tissues were washed in PBS and embedded in 2% agarose/PBS. Each slice was transferred to an individual well of a 24-well plate and reacted with the LR-1 antiserum (kindly provided by Dr Robert Benoit, McGill University, Montreal, Quebec, Canada) at a dilution of 1:10 000. Bound antibody was visualized as described (Kruger and Braun, 2002). Detection of β-galactosidase activities by whole-mount X-Gal staining was performed as reported (Kruger and Braun, 2002). For double labeling, frozen sections were initially stained for β-galactosidase activity followed by the appropriate immunostaining. Whole-mount *in situ* hybridization on free floating and cryosections was performed as described (Mennerich and Braun, 2001). The necdin antisense probe was synthesized from a 1.5 kbp cDNA fragment using T3 RNA polymerase. Statistical analysis was performed with Student's *t*-test. The level of significance was set at $P<0.05$. Data were presented as mean ± standard error of the mean. Usually three pairs of wild-type and mutant mice for each developmental stage were counted for GnRH-1-positive neurons ($n=3$).

Plasmids, cell culture, and transfections

The coding regions of mouse NSCL-2, LMO-1, LMO-2, and LMO-4 were cloned into the eukaryotic expression vector pCS2 + MT (Mennerich and Braun, 2001). For efficient *in vitro* transcription/translation, cDNAs for NSCL-1/2, E12, and LMO were inserted into pT7β-Sal (Braun and Arnold, 1991). The reporter construct pTA-Luc-NP was constructed by insertion of the 5′-flanking region (−844 to +63) of the necdin gene, which was obtained by PCR amplification using genomic mouse DNA, into the *Xho*I site of pTA-Luc (Clontech). The reporter constructs pTA-Luc-NPbox1, -box2, and -box1, 2, which carry mutations in E-box1, E-box2, and in both E-boxes of the mouse necdin promoter, were generated using the Quick Change Site-Directed Mutagenesis Kit according to the instructions of the manufacturer (Stratagene). E-box1 was mutated from CATGTG to TCGGTG, and E-box2 from CACATG to TGAATG. The expression vector for E12 has been described before (Braun *et al*, 1990). HEK293T cells were cultured in Dulbecco's modified Eagle's medium (DMEM) with 10% FCS and transfected with 2 μg of different expression vectors containing either NSCL-1, NSCL-2, E12, LMO-1, LMO-2, LMO-4, or pCS2MT-CLIM2 (Ostendorff *et al*, 2002) together with the reporter construct pTA-Luc-NP as described (Braun *et al*, 1990). Hypothalamic GT1-*trk* cells were cultured in DMEM with 10% horse serum and transfected using the Fugene6 reagent (Roche). At 48 h after transfection, cells were harvested and luciferase activity was determined. Transfection efficiencies were normalized to a cotransfected β-Gal expression construct (pCMV-βGal). Relative light units were measured using a standard luminometer. The average of three independent experiments was shown.

Electrophoretic mobility shift assay

Sequences of oligonucleotides derived from the necdin promoter and used for band shift assays were as follows: E-box1 GGGCCCTCATT-TTCATGTGGGGCCTGGGGG; E-box2 GGCATT CAAATCTCACATGGATTTATCTCC. For competition experiments, different oligonucleotides with mutated E-boxes were used: E1mut GG-ATGGGTGCGTGGGGCC; E2mut GGAACAGACTATGGATTT. NSCL-2-myc protein was synthesized by coupled *in vitro* transcription/translation using the TNT System (Promega). Protein/DNA complexes were resolved using a 4% native polyacrylamide gel in 0.5 × TBE buffer.

Chromatin immunoprecipitation

293T or GT-1 cells were transfected with NSCL-2, E12, CLIM2, and LMO-4 or with pCS2MT as a negative control. At 48 h after transfection, 10^7 cells were collected in culture medium. Protein–DNA complexes were crosslinked with 1% formaldehyde for 15 min at room temperature and quenched with 36 mM glycine for 5 min. Cells were washed with TBS, collected by centrifugation, resuspended in RIPA buffer with protease inhibitors, and passed several times through a 21-gauge needle. Chromatin was sheared by sonication. Cleared extracts were incubated with Protein G Sepharose (Amersham Biosciences) to reduce unspecific binding. Immunoprecipitation was carried out with the aid of a monoclonal antibody against the c-myc epitope (clone 9E10) and Protein G Sepharose. Beads were washed four times in RIPA buffer, RIPA, LiCl/detergent solution, and TBS. After elution of immunoprecipitates with 1% SDS/TE, crosslinking was reversed by incubation at 65°C for 6 h. Proteinase K-treated samples were cleared by phenol/chloroform extraction and DNA was precipitated. Precipitated chromatin regions were identified by PCR using primers that flank the two E-boxes of the mouse necdin gene (in the case of GT1-trk cells) resulting in a 277 bp fragment (primer 1: CAACAAACTGAG CATCCAATGA; primer 2: GAATGCAGATCAAACAAGC-AAGA), or primers that flank the second E-box of the human necdin gene (in the case of 293T cells) resulting in a 276 bp fragment (primer 1: CTGGGCAGAGGGAAAAGACAT; primer2: ATCGACTCCCTACCAAAT CAGA). PCR products were cloned and verified by sequence analysis.

Supplementary data

Supplementary data are available at *The EMBO Journal* Online.

Acknowledgements

We are indebted to Robert Benoit (McGill University, Montreal, Quebec, Canada) for kindly supplying the LR-1 antibody and to Ingolf Bach (ZMN Hamburg) for the generous gift of pCS2MT-CLIM2. We thank Daniel Spergel (University of Chicago) for helpful discussions and Eva Bober for critically reading the manuscript. This work was supported by the Deutsche Forschungsgemeinschaft, the 'Fonds der Chemischen Industrie', and the Wilhelm-Roux-Program for Research of the Martin-Luther-University.

References

Barker PA, Salehi A (2002) The MAGE proteins: emerging roles in cell cycle progression, apoptosis, and neurogenetic disease. *J Neurosci Res* **67:** 705–712

Braun T, Arnold HH (1991) The four human muscle regulatory helix–loop–helix proteins Myf3–Myf6 exhibit similar hetero-dimerization and DNA binding properties. *Nucleic Acids Res* **19:** 5645–5651

Braun T, Winter B, Bober E, Arnold HH (1990) Transcriptional activation domain of the muscle-specific gene-regulatory protein myf5. *Nature* **346:** 663–665

Bulchand S, Subramanian L, Tole S (2003) Dynamic spatiotemporal expression of LIM genes and cofactors in the embryonic and postnatal cerebral cortex. *Dev Dyn* **226:** 460–469

Cogliati T, Good DJ, Haigney M, Delgado-Romero P, Eckhaus MA, Koch WJ, Kirsch IR (2002) Predisposition to arrhythmia and autonomic dysfunction in Nhlh1-deficient mice. *Mol Cell Biol* **22:** 4977–4983

Corradi A, Croci L, Broccoli V, Zecchini S, Previtali S, Wurst W, Amadio S, Maggi R, Quattrini A, Consalez GG (2003) Hypogonadotropic hypogonadism and peripheral neuropathy in Ebf2-null mice. *Development* **130:** 401–410

Coyle CA, Jing E, Hosmer T, Powers JB, Wade G, Good DJ (2002) Reduced voluntary activity precedes adult-onset obesity in Nhlh2 knockout mice. *Physiol Behav* **77:** 387–402

Gerard M, Hernandez L, Wevrick R, Stewart CL (1999) Disruption of the mouse necdin gene results in early post-natal lethality. *Nat Genet* **23:** 199–202

Good DJ, Porter FD, Mahon KA, Parlow AF, Westphal H, Kirsch IR (1997) Hypogonadism and obesity in mice with a targeted deletion of the Nhlh2 gene. *Nat Genet* **15:** 397–401

Heger S, Seney M, Bless E, Schwarting GA, Bilger M, Mungenast A, Ojeda SR, Tobet SA (2003) Overexpression of glutamic acid decarboxylase-67 (GAD-67) in gonadotropin-releasing hormone neurons disrupts migratory fate and female reproductive function in mice. *Endocrinology* **144:** 2566–2579

Hosoya T, Oda Y, Takahashi S, Morita M, Kawauchi S, Ema M, Yamamoto M, Fujii-Kuriyama Y (2001) Defective development of secretory neurones in the hypothalamus of Arnt2-knockout mice. *Genes Cells* **6:** 361–374

Jay P, Rougeulle C, Massacrier A, Moncla A, Mattei MG, Malzac P, Roeckel N, Taviaux S, Lefranc JL, Cau P, Berta P, Lalande M, Muscatelli F (1997) The human necdin gene, NDN, is maternally imprinted and located in the Prader–Willi syndrome chromosomal region. *Nat Genet* **17:** 357–361

Johnson JD, Zhang W, Rudnick A, Rutter WJ, German MS (1997) Transcriptional synergy between LIM-homeodomain proteins and basic helix–loop–helix proteins: the LIM2 domain determines specificity. *Mol Cell Biol* **17:** 3488–3496

Kobayashi M, Taniura H, Yoshikawa K (2002) Ectopic expression of necdin induces differentiation of mouse neuroblastoma cells. *J Biol Chem* **277:** 42128–42135

Kruger M, Braun T (2002) The neuronal basic helix–loop–helix transcription factor NSCL-1 is dispensable for normal neuronal development. *Mol Cell Biol* **22:** 792–800

Lipkowitz S, Gobel V, Varterasian ML, Nakahara K, Tchorz K, Kirsch IR (1992) A comparative structural characterization of the human NSCL-1 and NSCL-2 genes. Two basic helix–loop–helix genes expressed in the developing nervous system. *J Biol Chem* **267:** 21065–21071

Lopez FJ, Merchenthaler IJ, Moretto M, Negro-Vilar A (1998) Modulating mechanisms of neuroendocrine cell activity: the LHRH pulse generator. *Cell Mol Neurobiol* **18:** 125–146

MacDonald HR, Wevrick R (1997) The necdin gene is deleted in Prader–Willi syndrome and is imprinted in human and mouse. *Hum Mol Genet* **6:** 1873–1878

Ma Q, Fode C, Guillemot F, Anderson DJ (1999) Neurogenin1 and neurogenin2 control two distinct waves of neurogenesis in developing dorsal root ganglia. *Genes Dev* **13:** 1717–1728

Mason AJ, Hayflick JS, Zoeller RT, Young III WS, Phillips HS, Nikolics K, Seeburg PH (1986) A deletion truncating the gonadotropin-releasing hormone gene is responsible for hypogonadism in the hpg mouse. *Science* **234:** 1366–1371

Mellon PL, Windle JJ, Goldsmith PC, Padula CA, Roberts JL, Weiner RI (1990) Immortalization of hypothalamic GnRH neurons by genetically targeted tumorigenesis. *Neuron* **5:** 1–10

Mennerich D, Braun T (2001) Activation of myogenesis by the homeobox gene Lbx1 requires cell proliferation. *EMBO J* **20:** 7174–7183

Michaud JL, Rosenquist T, May NR, Fan CM (1998) Development of neuroendocrine lineages requires the bHLH-PAS transcription factor SIM1. *Genes Dev* **12:** 3264–3275

Murdoch JN, Eddleston J, Leblond-Bourget N, Stanier P, Copp AJ (1999) Sequence and expression analysis of Nhlh1: a basic helix–loop–helix gene implicated in neurogenesis. *Dev Genet* **24:** 165–177

Muscatelli F, Abrous DN, Massacrier A, Boccaccio I, Le Moal M, Cau P, Cremer H (2000) Disruption of the mouse Necdin gene results in hypothalamic and behavioral alterations reminiscent of the human Prader–Willi syndrome. *Hum Mol Genet* **9:** 3101–3110

Nilaweera KN, Ellis C, Barrett P, Mercer JG, Morgan PJ (2002) Hypothalamic bHLH transcription factors are novel candidates in the regulation of energy balance. *Eur J Neurosci* **15:** 644–650

Ostendorff HP, Peirano RI, Peters MA, Schluter A, Bossenz M, Scheffner M, Bach I (2002) Ubiquitination-dependent cofactor exchange on LIM homeodomain transcription factors. *Nature* **416:** 99–103

Schafer K, Braun T (1999) Early specification of limb muscle precursor cells by the homeobox gene Lbx1h. *Nat Genet* **23:** 213–216

Schatzl HM, Laszlo L, Holtzman DM, Tatzelt J, DeArmond SJ, Weiner RI, Mobley WC, Prusiner SB (1997) A hypothalamic neuronal cell line persistently infected with scrapie prions exhibits apoptosis. *J Virol* **71:** 8821–8831

Schwab MH, Druffel-Augustin S, Gass P, Jung M, Klugmann M, Bartholomae A, Rossner MJ, Nave KA (1998) Neuronal basic helix–loop–helix proteins (NEX, neuroD, NDRF): spatiotemporal expression and targeted disruption of the NEX gene in transgenic mice. *J Neurosci* **18:** 1408–1418

Schwanzel-Fukuda M, Pfaff DW (1989) Origin of luteinizing hormone-releasing hormone neurons. *Nature* **338:** 161–164

Taniura H, Matsumoto K, Yoshikawa K (1999) Physical and functional interactions of neuronal growth suppressor necdin with p53. *J Biol Chem* **274:** 16242–16248

Tcherpakov M, Bronfman FC, Conticello SG, Vaskovsky A, Levy Z, Niinobe M, Yoshikawa K, Arenas E, Fainzilber M (2002) The p75 neurotrophin receptor interacts with multiple MAGE proteins. *J Biol Chem* **277:** 49101–49104

Treier M, Rosenfeld MG (1996) The hypothalamic-pituitary axis: co-development of two organs. *Curr Opin Cell Biol* **8:** 833–843

Tsai TF, Armstrong D, Beaudet AL (1999) Necdin-deficient mice do not show lethality or the obesity and infertility of Prader–Willi syndrome. *Nat Genet* **22:** 15–16

Uetsuki T, Takagi K, Sugiura H, Yoshikawa K (1996) Structure and expression of the mouse necdin gene. Identification of a postmitotic neuron-restrictive core promoter. *J Biol Chem* **271:** 918–924

Wray S, Grant P, Gainer H (1989) Evidence that cells expressing luteinizing hormone-releasing hormone mRNA in the mouse are derived from progenitor cells in the olfactory placode. *Proc Natl Acad Sci USA* **86:** 8132–8136

Wu TJ, Gibson MJ, Rogers MC, Silverman AJ (1997) New observations on the development of the gonadotropin-releasing hormone system in the mouse. *J Neurobiol* **33:** 983–998

Yoshikawa K (2000) Cell cycle regulators in neural stem cells and postmitotic neurons. *Neurosci Res* **37:** 1–14